

Contributions of first-principles calculations to explaining structure-property relationships in perovskites

Eric Cockayne

Ceramics Division, Materials Science and Engineering Laboratory,

National Institute of Standards and Technology,

Gaithersburg, Maryland 20899-8520

(Dated: April 1, 2008)

Abstract

This article discusses the contribution of first principles calculations toward explaining structure-property relationships in perovskites. In particular, the modern theory of polarization has helped to establish the origin of the large dynamical charges in perovskites. These large dynamical charges, along with the softness of the perovskite structure toward distortion, are the common origin of the high dielectric permittivities and piezoelectric coefficients observed in many perovskites. Effective Hamiltonians based on first principles calculations have been used to model the temperature dependent behavior of perovskite solid solutions. In solid solutions, sufficiently strong and inhomogeneous local fields can produce relaxor-ferroelectric-like behavior

PACS numbers:

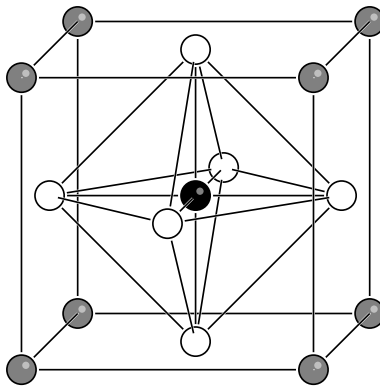


FIG. 1: The perovskite structure. The perovskite A site is shown in gray, the B site in black, and the O sites in white. Typically, the A site is occupied by a large, lower-valence cation, and the B site by a small, higher-valence cation. Solid solutions are possible by mixing the atomic species on the A sublattice, the B sublattice, or both.

I. INTRODUCTION

Many of the largest dielectric and piezoelectric constants occur in materials with the perovskite structure (Fig. 1), in particular, structures with two or more different chemical species on one of the sublattices[1]. It would thus be useful to have predictive tools for how the cation arrangements within the perovskite structure affect the temperature-dependent physical properties. Experiment, theory, and computation have all contributed toward understanding the basis of structure-property relationships in perovskites. This paper discusses the contribution of first-principles calculations, and models based on first-principles calculations. The topics covered range from the origin of the high dielectric permittivities to effective Hamiltonian models for temperature-dependent behavior in simple and complex perovskites.

Along with the above-mentioned dielectric and piezoelectric phenomena, materials with the perovskite structure are also known to exhibit interesting magnetic[2] and multiferroic[3] behaviors. This paper focuses on structural, dielectric and piezoelectric properties of non-magnetic perovskites.

II. FIRST-PRINCIPLES CALCULATIONS

Ultimately, the structure, stability, excitations, and response of a solid to external fields are determined by its electronic structure. The electronic structure problem has a very simple form

$$H\Phi = E\Phi, \tag{1}$$

where Φ is the many-body wavefunction, H the Hamiltonian and E the total energy. First principles methods are those that calculate electronic structures and properties derived from the electronic structure by solving Eq. (1). Unfortunately, Eq. (1) can only be solved exactly for simple systems, such as the hydrogen atom. Even worse, numerical solution is not simple either, due to electronic correlations which preclude a compact and accurate description of the electronic wavefunction, and to the fermion nature of electrons, which constrains the total wavefunction to change sign when any two electrons of like spin are exchanged.

All current first-principles solutions for large systems thus have some error. Various methods exist for approximately solving Eq. (1). Quantum Monte Carlo[4] is a powerful method, because it does determine the correct electronic structure of ground states. It does so, however, in a statistical way, and it is not a practical method at present to study systems with as many electrons per unit cells as perovskites have. Currently, the most efficient and widely used first-principles methods for problems in perovskites use density functional theory.

Density functional theory (DFT) is based on the Hohenberg-Kohn theorem[5]. This theorem states that the electronic structure problem can be reformulated in a way that depends on the electronic density $\rho(\mathbf{r})$ rather than the many-body wavefunction. The energy is then a functional of the electronic density and external potential. Minimizing this functional gives both the ground state charge density and the ground state energy correctly.

Kohn and Sham[6] found a practical way of implementing DFT, based on writing the total charge density in terms of one-electron wavefunctions and solving for these wavefunctions in a self consistent way. While, in principle, DFT is exact, it is not in practice, because the exact density functional is unknown. The unknown part is associated with the contribution of exchange and correlation to the energy. Practical applications of DFT include an exchange-correlation part of the functional, F_{xc} that is designed to approximate the exact and unknown true exchange-correlation functional. Two of the most commonly used approximations are

the local density approximation (LDA), with an F_{xc} that only depends on the local electronic density, and the generalized gradient approximation (GGA), which includes information from both the local density and the local charge gradient. Defects of results based on these approximations are well known. The lattice parameters found using LDA are commonly too small, those found using GGA are generally too large, and both give bandgaps for insulators that are too small. Perhaps surprisingly, on the whole, the LDA seems to work as well or better for perovskites than the GGA, even though one would think that the GGA is “better” because it includes more information.

In addition to electronic structure and total energy, density functional theory can be used to calculate the response of a crystal to various perturbations[7]. Density functional perturbation theory has been developed for these purposes. According to the $2N + 1$ theorem[8], perturbation of the DFT wavefunctions to order N allow for derivatives of the total energy to be calculated to order $2N + 1$ with respect to one or more perturbation. Examples of the useful perturbations and their associated response quantities include displacement (force constant), strain (stress), and external electric field (polarization), combined displacement and electric field (dynamic ionic charges). First-principles calculations of polarization, effective charges, and force constants are used to calculate the dielectric response as described in Sec. III C. Application of DFT to problems in materials science is widespread due to the wide availability of DFT codes and the speed of current microprocessors.

III. RESULTS

A. Perovskite phase stability

The issues of perovskite phase stability can be viewed at several levels: the stability of the perovskite phase in a system with respect to non-perovskite polymorphs, the relative stability of different orderings of cations in disordered perovskites with the associated phenomena of order/disorder transitions, phase separation, *etc.*, and the *structural* phase transitions of the perovskite phase between the cubic phase and various broken symmetry phases such as ferroelectric phases or those with oxygen octahedral tilting. The stability of solid solutions is discussed in Sec. III E.

Looking at the perovskite as a mix between the A-O and B-O endmember perovskites,

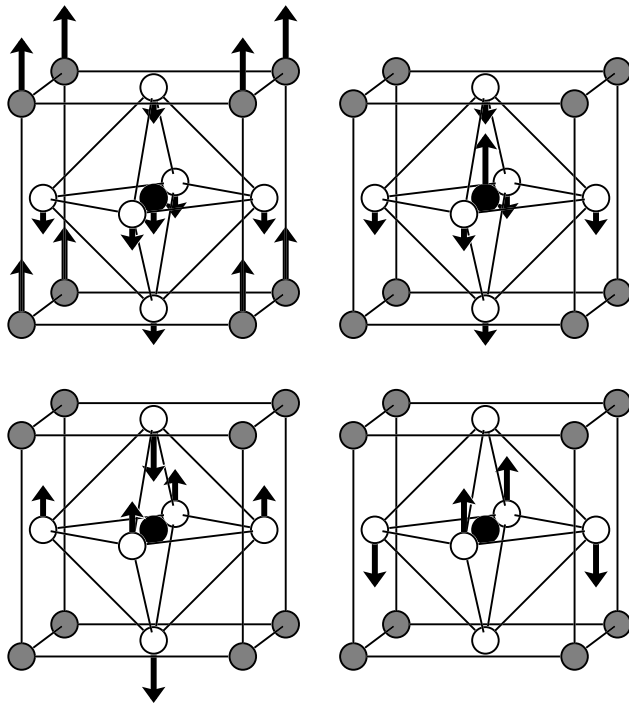


FIG. 2: Four optical modes of the primitive perovskite cell. (Top left) Last (Top right) Slater (Bottom left) octahedral stretching (Bottom right) Silent. The first three modes are infrared active and Raman silent, the last is both infrared-silent and Raman-silent.

the perovskite phase usually has a narrow stability region due to the very different nature of the A-O and B-O phases and the sensitive charge balances required for perovskite. The perovskite phase itself may not be the lowest energy polymorph for that stoichiometry. While this is generally of only incidental interest to how the perovskite structure affects the physical properties, it is an important consideration for some problems. For example, although the perovskite phase of MgSiO_3 is not stable at atmospheric pressure, it is believed to be stabilized at the high pressures that occur in the earth's interior[9]. Also, the PbTiO_3 - BiScO_3 solid solution is important because it has a high Curie temperature at the morphotropic phase boundary[10], although the “endmember” compound BiScO_3 is not stable in the perovskite phase[11].

The majority of perovskites have ground states that are distortions of the ideal cubic structure. Traditionally, the most common distortions have been explained in terms of the Goldschmidt tolerance factor[12]

$$t = \frac{r_A + r_O}{\sqrt{2}(r_B + r_O)}. \quad (2)$$

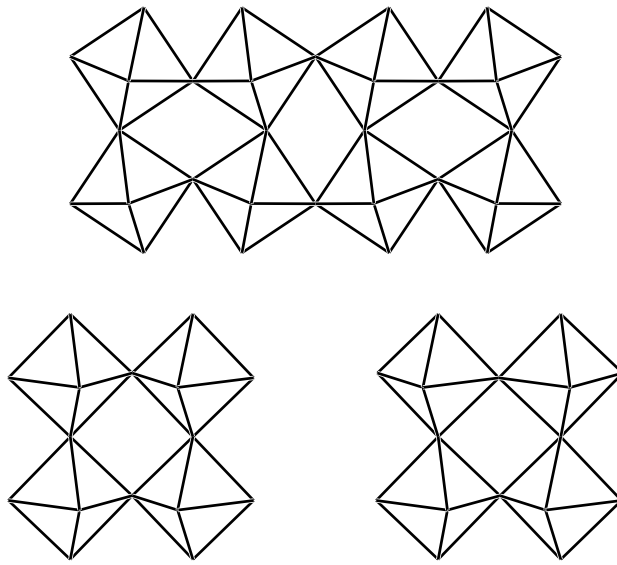


FIG. 3: (a) top view of octahedral tilting in the xy plane (b) side view of octahedral tilting corresponding to the M point in the Brillouin zone (c) side view of octahedral tilting corresponding to the R point in the Brillouin zone

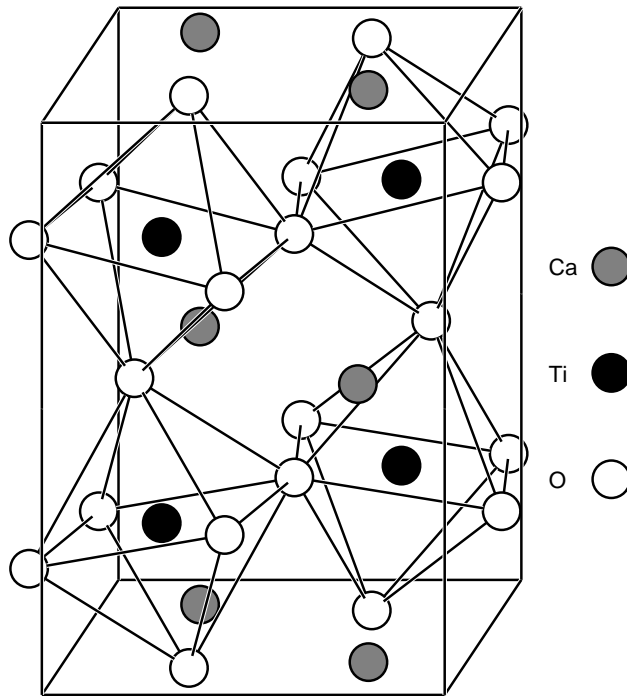


FIG. 4: Structure of CaTiO_3 , exhibiting octahedral tilting.

When $t > 1$, the ion on the B sublattice is “too small” and the structure is stabilized by ferroelectric off-center displacements of the B ion as represented by the Slater mode in Fig. 2. When $t < 1$, the ion on the A sublattice is “too small”, and the structure is generally stabilized by octahedral tilting, as shown in Fig. 3.

First principles normal mode calculations show that reality is more complicated. There are typically multiple instabilities present for perovskites, and one or more of these “competing instabilities” [13] wins to give the ground state. For example, the ground state of CaTiO_3 (Fig. 4) is produced by a mixture of M and R type octahedral tilting instabilities. The normal mode dispersion across the Brillouin for PbTiO_3 (Ref. 14) (Fig. 5) is representative of the complexity. Although the ground state is ferroelectric, the lowest branch between R and M is also unstable, demonstrating that ferroelectric and octahedral tilting compete. Note also, the relative flatness of the unstable band between R and M . This indicates that the R and M tilting have almost the same energy. In other words, the interplanar forces between the planes of tilted octahedra are weak [14]. In a similar way, the shape of the ferroelectric bands throughout the Brillouin zone has been used to explain the chainlike real space instabilities in KTaO_3 [15] that were suggested by experiment [16].

Further insight into the physics of the ferroelectric transition is obtained by looking at forces in real space. Cohen showed [17] how ferroelectricity is due to a sensitive balance between long range cubic forces and short range interatomic repulsions. Ti 3d - O 2p hybridization was found to be essential for ferroelectricity, The different ground state symmetries of BaTiO_3 and PbTiO_3 were explained by the chemical differences between Ba and Pb.

B. Dynamical effective charges

The influence of the dynamic effective charge of an ion to the response properties is so fundamental that we begin by reviewing basics of dielectric and piezoelectric response. The static dielectric response of a material is a tensor $\vec{\kappa}_s$, given by the change in polarization \vec{P} under an applied electric field \vec{E} :

$$(\kappa_s)_{\alpha\beta} = 1 + \frac{1}{\epsilon_0} \frac{\partial P_\alpha}{\partial E_\beta} \quad (3)$$

For simplicity, we derive the expression for the dielectric constant of a toy model consisting

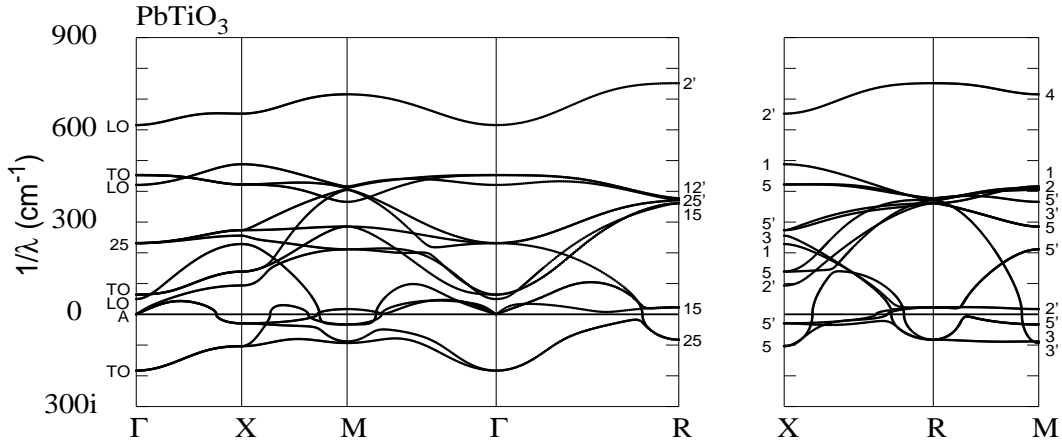


FIG. 5: Calculated normal mode dispersion for cubic PbTiO_3 .

of a mass m with charge Z on a spring with spring constant C inside a box of volume V . The spring is oriented along the z direction and we only consider the dielectric response to a field along z , reducing the dielectric tensor to a single component.

The force when an electric field E is applied is ZE . The displacement of the mass is thus $u = ZE/C$. The change in polarization is $\Delta P = (1/V)Zu = Z^2E/(CV)$. From Eq. (3),

$$\kappa_s = \frac{1}{V\epsilon_0} \frac{Z^2}{C}. \quad (4)$$

Now the (angular) frequency of oscillation of this mass on a spring is $\omega = \sqrt{C/m}$. The dielectric permittivity can be rewritten

$$\kappa_s = \frac{1}{V\epsilon_0} \frac{Z^2}{m\omega^2}. \quad (5)$$

The piezoelectric coefficient d is defined as

$$d = \frac{\partial P}{\partial \epsilon}, \quad (6)$$

where ϵ is the strain and P the polarization along z . In the toy model, the polarization is $(1/V)Zu_{eq}$, where u_{eq} is the equilibrium position of the ion; thus

$$d = \frac{1}{V} \left(Z \frac{\partial u_{eq}}{\partial E} + u_{eq} \frac{\partial Z}{\partial V} \right). \quad (7)$$

Real crystals are analogous, except that (1) they are three dimensional, thus strain, dielectric response, etc. are tensors; (2) the forces are chemical forces between atoms, not springs; (3) where the unit cell has a basis, there can be multiple polar modes; then Eq. (5)

has a sum over polar phonons; (4) there is an electronic contribution to the polarization, the polarization that would occur under an applied field if the ions were clamped; (5) the charges Z that act are not static charges, but are the dynamical charges Z^* , defined via the change in polarization as the individual ion i undergoes a displacement \vec{u}_i :

$$Z_{i\alpha\beta}^* \equiv \frac{\partial P_\alpha}{\partial u_{i\beta}}. \quad (8)$$

Because the effective charges that influence the dielectric and piezoelectric response are dynamic, not static, they can have values that are larger than their nominal ionic values. As early as 1967[18], there were experimental indications of anomalous effective charges in perovskites. In retrospect, the results were essentially correct; however, quantitative experimental determination of the Z^* is difficult because it presumes knowledge of the exact eigenvectors of all three perovskite infrared-active modes (Fig. 2).

Theoretical confirmation of the anomalous charges in perovskites awaited the modern theory of polarization. According to the modern theory of polarization[19], the polarization of a periodic solid is only defined in terms of the change of polarization with respect to a reference structure upon an adiabatic transformation. For perovskites and many other materials, the obvious reference structure is the high-symmetry ideal cubic perovskite state for which the polarization is zero. In turn, the polarization is defined in terms of an effective “Berry’s phase” involving the *phases* of the quantum mechanical wavefunctions. The traditional notion of polarization in an ionic solid as related to the charge *distribution* (see, *e.g.* chapter 27 of Reference 20) is invalid, because it is possible in principle for two different compounds to have the same charge distribution, but different polarizations with respect to their nonpolar reference structures.

Calculations of the Born effective charges in terms of the atomic wavefunctions calculated in density functional theory calculations became possible through the method given by King-Smith and Vanderbilt[21]. Using this method, the Born effective charges of a variety of perovskites was studied[22]. The results showed systematic anomalies, especially for ions on the perovskite B site that are polarizable (Ti, Ta, Zr, Nb), and for Pb on the perovskite A site. The origin of these large charges has been the subject of careful research[23]. The results favor a delocalized picture: movement of one ion causes the transfer of charges to and from other ions. This is especially true for the B-O bond when the B ion is highly polarizable. Eq. (5) shows that large dielectric and piezoelectric response can occur if Z^*

is large. First principles calculations have shown that this effect is common in compounds with the perovskite structure.

C. Dielectric and piezoelectric response

The full expression for the dielectric response of a crystal in terms of its phonon properties is given by

$$\kappa_{\alpha\beta} = (\kappa_{\infty})_{\alpha\beta} + \sum_{\mu} \frac{\overline{Z}_{\mu\alpha}^* \overline{Z}_{\mu\beta}^*}{V \epsilon_0 m_0 \omega_{\mu}^2}, \quad (9)$$

where $\vec{\kappa}_{\infty}$ is the electronic dielectric tensor, μ labels the zone-center ($\mathbf{q} = 0$) infrared-active normal modes of the system, ω_{μ} their (angular) frequencies, $\overline{Z}_{\mu\alpha}^*$ their effective charges in Cartesian direction α , and V the volume per unit cell. Note the similarity to Eq. (5).

An early application of this formula to a high-permittivity material was the study of Lee *et al.*[24] on non-perovskite rutile TiO_2 . Most early studies on the dielectric properties of perovskites focused on the dielectric peaks associated with ferroelectric phase transitions. These phenomena are discussed in Sec. III D. Non-ferroelectric such as SrTiO_3 and CaTiO_3 can also exhibit large dielectric constants ($\kappa_s > 100$). In Ref. 25, Eq. (9) was used to calculate the dielectric constant of CaTiO_3 . It was shown that the large permittivity arises from a relatively soft phonon with a large polarization associated with the large effective charge of Ti.

The usefulness of perovskites such as $\text{PbZr}_{1-x}\text{Ti}_x\text{O}_3$ (PZT) as transducers and actuators stems from their large piezoelectric coefficients. Naturally the origin of these large coefficients was studied from first-principles once the modern theory of polarization was developed. Sághi-Szabó *et al.* calculated the piezoelectric coefficients of PbTiO_3 and PZT[26], but the origin of the especially high response in PZT remained a puzzle. Fu and Cohen proposed that the large piezoelectric coefficients were associated with a “polarization rotation” mechanism[27]. For example, applying a [001] electric field to a crystal whose spontaneous polarization was in the [111] direction could “rotate” the polarization into the [aab] direction with a larger change in strain than applying an electric field of the same magnitude in the [111] direction. With a multidomain sample, it would even be possible to pole the system so that various $[\pm 1 \pm 1 1]$ domains gave an overall [001] polarization and polarization rotations

of the individual domains could occur in tandem, producing a large axial response that is actually due to polarization rotation.

D. Modeling temperature-dependent properties

Many perovskites exhibit temperature-dependent phase transitions such as transitions from ferroelectric to paraelectric states or between different ferroelectric phases. In these perovskites and even in others such as CaTiO_3 that do not undergo a transition at low temperatures, the temperature dependence of the dielectric response is very large. Understanding the temperature dependence of properties is very important for applications. In some cases, for example, one may want to tune the temperature of a dielectric constant maximum to some desired value. In other applications, such as microwave dielectric resonators, industrial specifications require that relative the *change* in the properties as the temperature changes be very small.

Fully first-principles molecular dynamics methods for calculating the time evolution of a structure at a given simulation temperature exist. Such methods give useful information about phonon frequencies, for example. For the kinds of large-scale simulations necessary to reproduce ferroelectric transitions and temperature-dependent dielectric permittivity, however, fully first-principles methods are not currently practical. Therefore, modeling based on first-principles results is used.

Several types of models are possible. One family of models is the “shell models”. In shell models, each atom is described by two charged particles: a massive core linked to a massless shell. There are Coulombic interactions between the core and shell of different atoms, and short-range interactions between shells. Shell models with parameters fitted from first-principles calculations offer a reliable atomic-level description of ferroelectric materials[28]. Temperature dependent properties can be obtained performing molecular dynamics simulations. The shell model has been extensively used and successfully shown to be able to describe properties of ferroelectric materials in bulk[29], thin films[30], superlattices[31], solid solutions[32], and interfaces[33].

To investigate the temperature-dependent dielectric permittivity of nonferroelectric perovskites, a simple model was devised where each individual polar phonon was represented by one independent uncoupled anharmonic oscillator per unit cell. In spirit, the model was

the anharmonic equivalent of the Einsteinian model for optical phonons in the harmonic crystal[20]. The anharmonic quantum oscillator problem was treated numerically as a function of temperature and applied electric field. In spite of the crudeness of this model, the relative trends of permittivity vs. temperature were correctly reproduced for CaTiO_3 and $\text{CaAl}_{1/2}\text{Nb}_{1/2}\text{O}_3$ [34].

A third approach to modeling temperature dependent properties of perovskites is the effective Hamiltonian approach. The effective Hamiltonian (H_{eff}) approach was devised to explore the problem of ferroelectric phase transitions in perovskites such as PbTiO_3 and BaTiO_3 (Refs. 35–38).

In H_{eff} , the full set of atomic displacements from equilibrium positions is projected onto the subspace of low-energy vibrational modes that includes the FE instabilities, represented by local variables $\vec{\xi}_i$ centered on the appropriate sublattice of the perovskite structure. H_{eff} is obtained from a Taylor expansion of the total energy around a high-symmetry reference structure in terms of $\vec{\xi}_i$ and homogeneous strain $e_{\alpha\beta}$:

$$H_{eff} = H(\vec{\xi}_i) + H(e_{\alpha\beta}) + H(\vec{\xi}_i, e_{\alpha\beta}) \quad (10)$$

The form of H_{eff} is convenient for calculating the temperature-dependent properties of perovskites via Monte Carlo or molecular dynamics simulations. The correct phase transitions or sequences of phase transitions are reproduced for BaTiO_3 and for PbTiO_3 , although the transition temperatures typically disagree with the experimental values because of the truncation of anharmonic terms in H_{eff} . The expressions for calculating dielectric permittivity and piezoelectric response within the H_{eff} approach have been derived[39], and the simulated temperature-dependent responses show large values near ferroelectric phase transitions.

E. Perovskite solid solutions

As discussed in the Introduction, the optimal properties of materials are often found in perovskite solid solutions. The composition of a solid solution can lead to effects that are not linear in the properties of the endmember compounds. More remarkably, the properties are sometimes more extreme than for either endmember compound, as is observed in $\text{Ba}_{1-x}\text{Sr}_x\text{CaO}_3$, where the dielectric constant is higher than that of either endmember compound[40, 41].

Furthermore, not only the composition of a solid solution, but also the degree to which the atomic species are ordered, can affect the physical properties. The dielectric constants in dielectrics whose cations are disordered can be 10 % to 20 % higher than of chemically ordered dielectrics of the same composition[42]. The changes in short range [Zn,Ta] chemical ordering in the commercial microwave dielectric $\text{BaZn}_{1/3}\text{Ta}_{2/3}\text{O}_3$ (BZT) as order 1 % to 10 % Zr and Ni are substituted is correlated with a 30 % reduction in dielectric loss relative to that of pure BZT[43]. Even more spectacular changes in physical properties vs. temperature as a function of ordering occur in Pb-based perovskite compounds, where high dielectric constants and piezoelectric coefficients persist over a wide temperature range in the so-called “relaxor state”. Here, experimental results[44] suggest that relaxor properties are correlated with chemically ordered domains of linear dimension roughly 2 nm to 5 nm embedded in a disordered matrix. When the $\text{PbSc}_{1/2}\text{Nb}_{1/2}\text{O}_3$ system has such local order, it exhibits a relaxor state between its high-temperature paraelectric and low temperature ferroelectric phases[45]. When the Sc and Nb have long-range order, however, there is no relaxor state.

Note that, solid solutions, while periodic on average, can not in general be represented by small enough unit cells to calculate their properties from first principles. They thus provide a natural set of problems for involving higher-level modeling such as cluster expansions. The cluster expansion technique has a long history. They were developed to model order-disorder phenomena in intermetallic compounds. The basic notion is quite simple: for a compound where two species A and B can occupy a single sublattice, one assigns the value $\sigma = 1$ or -1 to each site i on the sublattice according to whether the site is occupied by A or B . In an analogous way to the Ising model, one can write the total energy in terms of the “spins” occupying the sites and their interaction parameter $\{J\}$:

$$E = E_o + \sum_i J_i \sigma_i + \sum_{ij} J_{ij} \sigma_i \sigma_j + \dots \quad (11)$$

Assuming that J converges in physically reasonable ways, one can calculate the energy E for some small set of ordered structures, solve for the J in some fashion, and use the results in a Monte Carlo simulation to simulate temperature-dependent order-disorder and phase separation phenomena. There has been much development of the mathematics of calculating the J . Some recent developments include the introduction of the concept of the cross-validation score metric to in effect determine the goodness of the fit, and the incorporation of this method and other concepts into an automatic toolkit for solving such

problems[46].

For problems of B site ordering in perovskites, the general experimental trend makes sense: the more the charge difference and/or size difference between B and B' changes, the greater the tendency toward ordered compounds. Order-disorder transitions can be observed. In $\text{PbSc}_{1/2}\text{Nb}_{1/2}\text{O}_3$, for example, the cations can achieve long-range order if they are annealed below the order-disorder transition temperature; if annealed above this temperature, the compound does not have long-range order. Note the importance of dynamics: to actually change cation ordering, the cations need to swap between different sites. Below an effective freezing temperature, typically of order 1000 K, such swaps are dynamically too slow to occur in experimental times.

The intriguing cases are between order and disorder, where FP calculations can predict an ordered ground state structure which can not be achieved experimentally by heat treatment (although atomic layer deposition methods may allow for such structures to be made). In $\text{CaZr}_{1-x}\text{Ti}_x\text{O}_3$, there is some size difference, but essentially no charge difference between Zr and Ti. FP calculations predict that the ground state structure for $x = 1/2$ will have Zr and Ti ordered in the rocksalt pattern. Experimentally, only weak short-range ordering has been achieved[47].

For most perovskite $\text{A}[\text{BB}']\text{O}_3$ solid solutions, the ground state structures are those expected based on the charges of B and B'. In contrast, for $\text{Pb}[\text{BB}']\text{O}_3$ solid solutions, the energy differences between the various orderings of B and B' are much less than would be expected based on the Coulomb interaction between the charges. This effect has been explained by the tendency of Pb to form covalent bonds with underbonded oxygens in contrast to more ionic ions such as Ba[48]. Indeed, careful first-principles investigations of the possible ground state for $\text{PbMg}_{1/3}\text{Nb}_{2/3}\text{O}_3$ show that the predicted ground state is not that expected from minimizing the Coulomb energy between the Mg and Nb, but one with a more complicated arrangement[49, 50].

The large and unusual temperature-dependence of the piezoelectric and dielectric response of relaxors is what makes them useful for applications such as transducers and actuators. Modeling the temperature-dependent response of relaxors combined the problems of solid solutions of this section with the temperature-dependence problem of the previous section. The most successful first-principles-based approach to this problem is a modification of the effective Hamiltonian approach for solid solutions[51, 52] The effective Hamiltonian

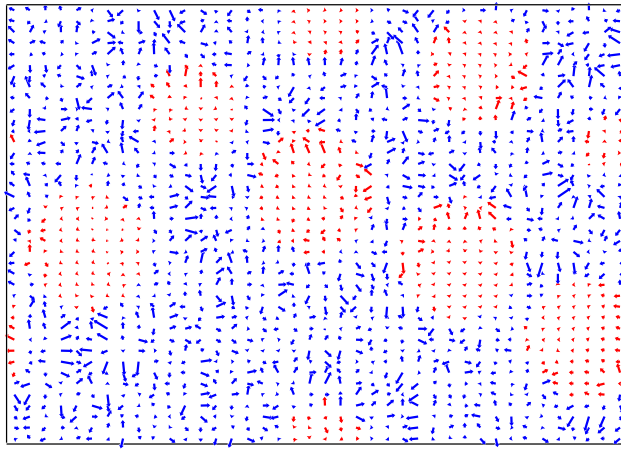


FIG. 6: Local “random” fields in (artificially) nanoscale chemically ordered PSN. In roughly spherical light (red in color figure) regions, the Sc and Nb are arranged with ideal rocksalt order; in dark (blue in color figure) regions, the Sc and Nb are arranged randomly. Note larger local fields in chemically random regions.

differs from that for a simple perovskite in containing a “random” local field term due to the disordered or partially disordered arrangement of B sites on the B site sublattice causing local electric or strain fields that differ from site to site. Fig. 6 shows the strength of the local electric fields that arise in $\text{PbSc}_{1/2}\text{Nb}_{1/2}\text{O}_3$ (PSN) due to the charge difference between the 3+ Sc and the 5 + Nb. The arrangement of the Sc and Nb has been set up to have nanoscale regions where the Sc and Nb have rocksalt ordering surrounded by regions where the Sc and Nb are placed randomly. Such a structure mimics that which has been observed experimentally to enhance the stability of the relaxor state[44].

Fig. 7 shows the results of a simulation of the effective Hamiltonian of the PSN model under a simulated 18 GPa pressure[53]. The histograms show the distribution of polarization of the nanoscale chemically ordered regions. There is a transition from the paraelectric phase to a relaxor phase to a ferroelectric ground state, similar to what is observed in PSN experimentally as a function of temperature. The relaxor state is characterized by nonzero polarization on the chemical ordered nanoregions, but no long range ferroelectric ordering, as shown by the bimodal distribution at 160 K. Furthermore, studies using the H_{eff} of [53] show that the temperature range of the relaxor state, or even the presence thereof, is enhanced in the case where the order on the B sublattice is inhomogeneous, in agreement with experiment.

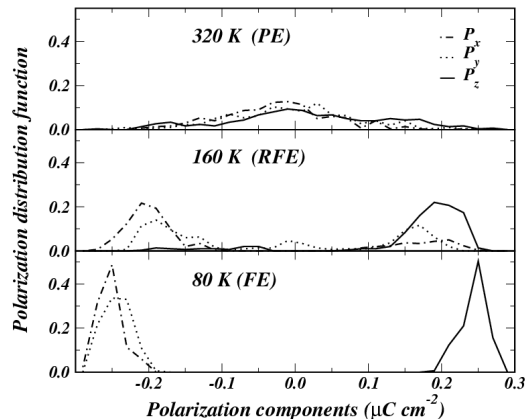


FIG. 7: Nanoscale chemically ordered polarization histogram as a function of temperature for the PSN effective Hamiltonian at 18 GPa.

F. Thin films and other nanostructured perovskites

Many applications and potential future applications of perovskites with useful physical properties will involve their use as thin films or in other nanoscale geometries. This raises several questions, including whether the properties of thin films are the same as those of bulk perovskites and whether new phenomena could occur in nanoscale perovskites. First-principles calculations have shed light on these issues.

The questions about whether thin films geometry affects the properties of ferroelectric perovskites relative to the bulk has been the subject of much first-principles research. One major question has been how thin can one make a thin film and still observe ferroelectricity. The results are found to depend on boundary conditions and the direction of polarization, but the trend of the results is to find that rather thin films can support ferroelectricity. For example, Ghosez and Rabe, using a first-principles based effective Hamiltonian, calculated that perpendicular ferroelectric polarization in PbTiO_3 under short-circuit boundary conditions could exist in films as thin as three perovskite layers[54]. Another issue that has been explored with first-principles energetic calculations and effective Hamiltonians is the temperature-strain phase diagram of thin film perovskites. Multiple phases are observed in these studies[55].

To see if nanoscale geometries such as nanodots could lead to unusual behavior, Naumov *et al.* looked at ferroelectric nanodots based on the PZT perovskite. They predicted a new

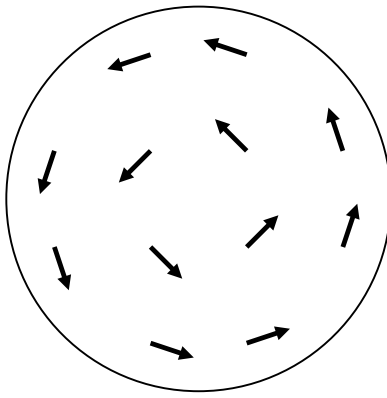


FIG. 8: Schematic of predicted local polarization in a ferroelectric nanodot.

kinds of phase transitions[56], involving chiral ordering of the local polarization (Fig. 8). Note that the polarization order parameter is the curl of the field. In principle, the sign of this chiral order parameter can be reversed. It is thus hypothesized that such nanoscale ferroelectrics could act as bits for passive or active storage in memory devices.

IV. CONCLUSIONS

First-principles calculations and models based on these calculations have shed light on the origins of a variety of phenomena associated with the perovskite structure and will continue to be a useful tool for investigating these complex and useful materials.

-
- [1] O. Madelung, ed., *Landolt-Börnstein Numerical Data and Functional Relationships in Science and Technology, New Series, volume 29b: Low Frequency Properties of Dielectric Crystals: Piezoelectric, Pyroelectric and Related Constants* (Springer-Verlag, Berlin, 1993).
 - [2] E. Dagotto, T. Hotta, and A. Moreo, *Phys. Rep.: Rev. Sect. Phys. Lett.* **344**, 1 (2001).
 - [3] J. Wang, J. B. Neaton, H. Zheng, V. Nagarajan, S. B. Ogale, B. Liu, D. Viehland, V. Vaithyanathan, D. G. Schlom, U. V. Waghmare, et al., *Science* **299**, 1719 (2003).
 - [4] D. M. Ceperley and B. Alder, *Science* **231**, 555 (1986).
 - [5] P. Hohenberg and W. Kohn, *Phys. Rev.* **136**, B864 (1964).
 - [6] W. Kohn and L. J. Sham, *Phys. Rev.* **140**, A1133 (1965).
 - [7] S. Baroni, S. de Gironcoli, A. D. Corso, and P. Giannozzi, *Rev. Mod. Phys.* **73**, 515 (2001).

- [8] X. Gonze and J.-P. Vigneron, *Phys. Rev. B* **39**, 13120 (1989).
- [9] S.-H. Shim, T. S. Duffy, and G. Shen, *Science* **293**, 2437 (2001).
- [10] R. E. Eitel, C. A. Randall, T. R. ShROUT, P. W. Rehrig, W. Hackenberger, and S.-E. Park, *Jpn. J. Appl. Phys.* **40**, 5999 (2001).
- [11] J. Íniguez, D. Vanderbilt, and L. Bellaiche, *Phys. Rev. B* **67**, 224107 (2003).
- [12] V. M. Goldschmidt, *Skrifter Norske Videnskaps-Akad. Oslo, I. Mat. Naturv.* pp. 8–8 (1926).
- [13] W. Zhong and D. Vanderbilt, *Phys. Rev. Lett.* **74**, 2587 (1995).
- [14] P. Ghosez, E. Cockayne, U. V. Waghmare, and K. M. Rabe, *Phys. Rev. B* **60**, 836 (1999).
- [15] R. Yu and H. Krakauer, *Phys. Rev. Lett.* **74**, 4067 (1995).
- [16] R. Comes, M. Lambert, and A. Guinier, *Solid State Commun.* **6**, 715 (1968).
- [17] R. E. Cohen, *Nature (London)* **358**, 136 (1992).
- [18] J. D. Axe, *Phys. Rev.* **157**, 429 (1967).
- [19] R. Resta, *Rev. Mod. Phys* **66**, 899 (1994).
- [20] N. W. Ashcroft and N. D. Mermin, *Solid State Physics* (Saunders College/Holt, Rinehart and Winston, Philadelphia, 1976).
- [21] R. D. King-Smith and D. Vanderbilt, *Phys. Rev. B* **47**, 1651 (1993).
- [22] W. Zhong, R. D. King-Smith, and D. Vanderbilt, *Phys. Rev. Lett.* **72**, 3618 (1994).
- [23] P. Ghosez, J.-P. Michenaud, and X. Gonze, *Phys. Rev. B* **58**, 6224 (1998).
- [24] C. Lee, P. Ghosez, and X. Gonze, *Phys. Rev. B* **50**, 13379 (1994).
- [25] E. Cockayne and B. P. Burton, *Phys. Rev. B* **62**, 3735 (2000).
- [26] G. Sági-Szabó, R. E. Cohen, and H. Krakauer, *Phys. Rev. B* **59**, 12771 (1999).
- [27] H. Fu and R. E. Cohen, *Nature (London)* **403**, 281 (2000).
- [28] M. Sepliarsky, A. Astahagiri, S. R. Phillpot, M. G. Stachiotti, and R. L. Migoni, *Curr. Opin. Sol. State Mater. Sci.* **9**, 107 (2005).
- [29] S. Tinte, M. G. Stachiotti, M. Sepliarsky, R. L. Migoni, and C. O. Rodriguez, *J. Phys.-Condens. Matter* **11**, 9679 (1999).
- [30] S. Tinte and M. G. Stachiotti, *Phys. Rev. B* **64**, 235403 (2001).
- [31] M. Sepliarsky, S. R. Phillpot, D. Wolf, M. G. Stachiotti, and R. L. Migoni, *Phys. Rev. B* **64**, R060101 (2001).
- [32] S. Tinte, M. G. Stachiotti, S. R. Phillpot, M. Sepliarsky, D. Wolf, and R. L. Migoni, *J. Phys.: Condens. Matter* **16**, 3495 (2004).

- [33] M. Sepiarsky, M. G. Stachiotti, and R. L. Migoni, *Phys. Rev. Lett.* **96**, 137603 (2006).
- [34] E. Cockayne, *J. Appl. Phys.* **90**, 1459 (2001).
- [35] K. M. Rabe and U. V. Waghmare, *Phys. Rev. B* **52**, 13236 (1995).
- [36] K. M. Rabe and U. V. Waghmare, *Ferroelectrics* **194**, 119 (1996).
- [37] U. V. Waghmare and K. M. Rabe, *Phys. Rev. B* **55**, 6161 (1997).
- [38] W. Zhong, D. Vanderbilt, and K. M. Rabe, *Phys. Rev. B* **52**, 6301 (1995).
- [39] K. M. Rabe and E. Cockayne, *AIP Conference Proc.* **436**, 61 (1998).
- [40] T. Yamaguchi, Y. Komatsu, T. Otobe, and Y. Murakami, *Ferroelectrics* **27**, 273 (1980).
- [41] I. Levin, T. G. Amos, S. M. Bell, L. Farber, T. A. Vanderah, R. S. Roth, and B. H. Toby, *J. Solid State Chem* **175**, 170 (2003).
- [42] R. J. Cava et al., *Mater. Res. Bull.* **534**, 355 (1999).
- [43] P. K. Davies, J. Tong, and T. Negas, *J. Am. Ceram. Soc.* **80**, 1727 (1997).
- [44] C. A. Randall and A. S. Bhalla, *Jpn. J. Appl. Phys.* **29**, 327 (1990).
- [45] F. Chu, I. M. Reaney, and N. Setter, *J. Appl. Phys.* **77**, 1671 (1995).
- [46] A. van de Walle, M. Asta, and G. Ceder, *CALPHAD: Comput. Coupling Phase Diagrams Thermochem.* **26**, 539 (2002).
- [47] V. Krayzman and I. Levin, *J. Appl. Crystallogr.* **41**, 386 (2008).
- [48] B. P. Burton and E. Cockayne, *Phys. Rev. B* **60**, R12542 (1999).
- [49] B. P. Burton, R. P. McCormack, B. H. Toby, and E. K. Goo, *Ferroelectrics* **194**, 187 (1997).
- [50] S. A. Prosandeev, E. Cockayne, B. P. Burton, S. Kamba, J. Petzelt, Y. Yuzyuk, R. S. Katiyar, and S. B. Vakrushev, *Phys. Rev. B* **70**, 134110 (2004).
- [51] R. Hemphill, L. Bellaiche, A. García, and D. Vanderbilt, *Appl. Phys. Lett.* **77**, 3642 (2000).
- [52] E. Cockayne, B. P. Burton, and L. Bellaich, *AIP Conference Proc.* **582**, 191 (2001).
- [53] S. Tinte, B. P. Burton, E. Cockayne, and U. V. Waghmare, *Phys. Rev. Lett.* **97**, 137601 (2006).
- [54] P. Ghosez and K. M. Rabe, *Appl. Phys. Lett.* **76**, 2767 (2000).
- [55] O. Dieguez, S. Tinte, A. Antons, C. Bungaro, J. B. Neaton, K. M. Rabe, and D. Vanderbilt, *Phys. Rev. B* **69**, 212101 (2004).
- [56] I. I. Naumov, L. Bellaiche, and H. Fu, *Nature (London)* **432**, 737 (2004).